

Optimized Tire Force Estimation using Extended Kalman Filter and Fruit Fly Optimization

Kanarachos, S, Acosta, M & Fitzpatrick, M

Author post-print (accepted) deposited by Coventry University's Repository

Original citation & hyperlink:

Kanarachos, S, Acosta, M & Fitzpatrick, M 2017, Optimized Tire Force Estimation using Extended Kalman Filter and Fruit Fly Optimization. in *43rd Annual Conference of the IEEE Industrial Electronics Society*. IEEE, pp. 4074-4079, 43rd Annual Conference of the IEEE Industrial Electronics Society, Beijing, China, 29-1 November <https://dx.doi.org/10.1109/IECON.2017.8216698>

DOI	10.1109/IECON.2017.8216698
Electronic ISBN	978-1-5386-1127-2
USB ISBN	978-1-5386-1126-5
Print on Demand ISBN	978-1-5386-1128-9

Publisher: IEEE

© 2017 IEEE. Personal use of this material is permitted. Permission from IEEE must be obtained for all other uses, in any current or future media, including reprinting/republishing this material for advertising or promotional purposes, creating new collective works, for resale or redistribution to servers or lists, or reuse of any copyrighted component of this work in other works.

Copyright © and Moral Rights are retained by the author(s) and/ or other copyright owners. A copy can be downloaded for personal non-commercial research or study, without prior permission or charge. This item cannot be reproduced or quoted extensively from without first obtaining permission in writing from the copyright holder(s). The content must not be changed in any way or sold commercially in any format or medium without the formal permission of the copyright holders.

This document is the author's post-print version, incorporating any revisions agreed during the peer-review process. Some differences between the published version and this version may remain and you are advised to consult the published version if you wish to cite from it.

Optimized Tire Force Estimation using Extended Kalman Filter and Fruit Fly Optimization

Manuel Acosta, Stratis Kanarachos, and Michael E. Fitzpatrick

School of Mechanical, Aerospace and Automotive Engineering

Coventry University

Coventry, U. K.

Email: ac3354@coventry.ac.uk; ab8522@coventry.ac.uk; ab6856@coventry.ac.uk

Abstract — This paper deals with the automated design of a Virtual Sensor used to estimate the vehicle planar motion states and the axle lateral forces. It is proposed to substitute the cumbersome and non-trivial manual task of tuning a Kalman Filter by using meta-heuristic optimization, and in particular, employing the contrast-based Fruit Fly Optimization Algorithm (c-FOA). c-FOA is a recently developed powerful Swarm Intelligence meta-heuristic. The optimized state estimator is implemented in the vehicle dynamics simulation software *IPG – CarMaker®* and its performance is evaluated under aggressive maneuvers. Results are compared to those obtained with a filter tuned manually in previous stages of this research using a systematic trial and error method.

Keywords—Tire Force Estimation: Extended Kalman Filter: Neural Networks: Fruit Fly Optimization

I. INTRODUCTION

The development of Modern Automotive Control Systems [1,2] requires the accurate and timely estimation of an elevated number of vehicle states [3,4] which cannot be directly measured. This approach, also called Virtual Sensing, is of great importance especially in the case of tire forces. Up to now, no commercially available sensors can directly measure the tire forces and relevant research has shown that various proposed approaches are too complex, expensive or unreliable to implement [5,6,7,8].

The standard method for vehicle state and tire force estimation is the Kalman Filter [9,10]. Different versions of Kalman filters exist including, the linear one, Extended Kalman Filter (*EKF*), Unscented Kalman Filter (*UKF*), and Particle Filters [11]. Since tire forces exhibit a smooth nonlinear behavior at high longitudinal slip ratios and lateral slip angles, the Extended Kalman Filter is commonly used to estimate the tire forces [12,13,14].

Tuning an Extended Kalman Filter, selecting the measurement and noise statistics, is a cumbersome process as it is a multivariable problem with competing objectives [15]. For the derivation of an adequate solution, a multiple parameter trade-off analysis – considering performance in steady state maneuvers, performance in dynamic maneuvers, root mean square (*RMS*) values, maximum absolute error – is required. There are no design rules in place which can be used for this complex purpose and current practice relies on trial and error

methods. A new trend is to tune the *EKF* using numerical optimization techniques [16, 17]. However, this approach has not been tested before in vehicle dynamics. Furthermore, it is not straightforward to apply numerical optimization, as the objective function is noisy and nonlinear. Thus, the application of gradient optimization techniques is not suitable. To this end, several authors proposed the application of Gaussian optimization [18].

In this paper, we propose the tuning of an Extended Kalman Filter used for tire force estimation, by applying the contrast-based Fruit Fly Optimization Algorithm (*c-FOA*) [19]. The numerical results obtained indicate the significant performance improvement of *EKF* compared to the standard systematic trial-and-error method. Furthermore, the authors provide insight into the application of *c-FOA* by proposing an objective function comprising a weighted combination of longitudinal velocity, lateral velocity, yaw rate and lateral acceleration errors. By incorporating the lateral acceleration error, the optimum solution is achieved more robustly and with fewer iterations compared to the standard objective function, comprising a combination of just the vehicle states.

The rest of the paper is organized as follows: In Section II, the structure of the tire force state estimator is presented. The vehicle model, the data-based approach to model the tire friction forces and the Extended Kalman Filter formulation are introduced. The optimization routine of the contrast-based Fruit Fly algorithm and the optimization objective function proposed in this paper are described in Section III. The results obtained after subjecting the optimized Extended Kalman Filter to Open Loop and Closed Loop aggressive dynamic maneuvers are discussed in Section IV. Finally, conclusions and further research steps are provided in Section V.

II. HYBRID OBSERVER STRUCTURE

The structure of the Hybrid observer proposed in this work is depicted in Fig. 1. As can be seen, the state estimator consists of an Extended Kalman Filter and a Feedforward Neural Networks (*NN*) block. The vehicle planar dynamics are modeled in the *EKF* by means of a Single Track vehicle model, whereas the axle lateral forces are approximated by a Static (1-10-1) *NN* structure. This hybrid modeling approach is advantageous compared to other “black-box” [20] or “tire model-based” [9] modeling techniques in the sense that no

prior knowledge of the tire model is assumed nor the vehicle dynamics are treated as a black box. Instead, it combines the advantages of the *NN* in modeling the tire's highly nonlinear behavior with a first principles model that captures the overall dynamic behavior.

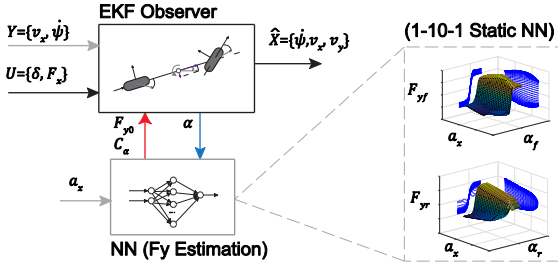


Fig. 1. Virtual Sensor Structure.

A. Vehicle Modeling

The vehicle planar dynamics are modeled using a Single Track model [21], Fig. 2.

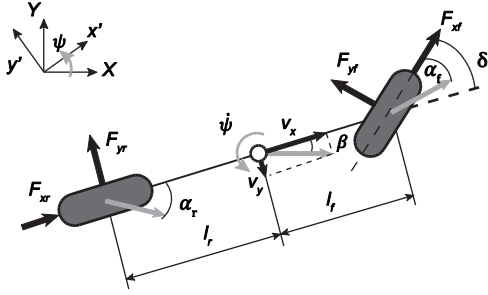


Fig. 2. Single Track vehicle model.

The longitudinal, lateral and rotational dynamic equilibrium equations are discretized using a first order approximation ($e^{AT_s} \approx 1 + AT_s$), and expressions (1-3) are obtained.

$$v_{x,k+1} = v_{x,k} + T_s \dot{\psi}_k v_{y,k} + \frac{T_s}{m} (F_{xf,k} \cos(\delta_k) - F_{yf,k} \sin(\delta_k) + F_{xr,k}) \quad (1)$$

$$v_{y,k+1} = v_{y,k} - T_s \dot{\psi}_k v_{x,k} + \frac{T_s}{m} (F_{yf,k} \cos(\delta_k) + F_{xf,k} \sin(\delta_k) + F_{yr,k}) \quad (2)$$

$$\dot{\psi}_{k+1} = \dot{\psi}_k + \frac{T_s}{I_\psi} (F_{yf,k} \cos(\delta_k) l_f + F_{xf,k} \sin(\delta_k) l_f - F_{yr,k} l_r) \quad (3)$$

Where T_s denotes the discretization time, l_f and l_r the distances from the center of gravity to the front and rear axles respectively, m the mass of the vehicle, and I_ψ the yaw inertia. The vector of states (X) is formed by the longitudinal velocity (v_x), the lateral velocity (v_y), and the yaw rate ($\dot{\psi}$), expression (4). The front and rear axle longitudinal forces (F_{xf}, F_{xr}) and

the angle steered by the front wheels (δ) are considered inputs to the system, expression (5). Finally, the yaw rate and longitudinal velocity quantities are assumed measurable variables, and form the vector of measurements (Y), equation (6).

$$X = \{v_x, v_y, \dot{\psi}\} \quad (4)$$

$$U = \{F_{xf}, F_{xr}, \delta\} \quad (5)$$

$$Y = \{v_x, \dot{\psi}\} \quad (6)$$

B. Tire Force Modeling

The nonlinear axle lateral forces (7) are approximated by a first order Taylor series expansion, and expression (8) is obtained.

$$F_y = f(\alpha, \lambda) \quad (7)$$

$$F_y \approx F_{y0} + \frac{\partial F_y}{\partial \alpha} \Delta \alpha + \frac{\partial F_y}{\partial \lambda} \Delta \lambda \quad (8)$$

The second derivative term is neglected under the assumption of quasi-static conditions in the longitudinal direction. The first derivative term (C , cornering stiffness) is approximated using a finite differences approach (9).

$$\frac{\partial F_y}{\partial \alpha} = C \approx \frac{F_{y,\alpha_0 + \Delta \alpha_t} - F_{y,\alpha_0 - \Delta \alpha_t}}{2 \Delta \alpha_t} \quad (9)$$

The term $\Delta \alpha_t$ denotes a small fixed axle slip increment, and is different from the increment ($\Delta \alpha$) presented in expression (8).

C. Neural Networks

A model-based approach [3,22] is used to determine the static lateral force (F_{y0}) and cornering stiffness (C) required to calculate the axle lateral forces, equation (8). The tire friction nonlinear behavior is approximated using a one-hidden-layer *NN* structure. The vehicle longitudinal acceleration (a_x) and the axle wheel slips (α) are selected as the *NN* inputs. The axle wheel slips are computed from the vehicle states using a small angle approximation [23], expressions (10-11).

$$\alpha_{f,k} = \delta_k - \left(\frac{\dot{\psi}_k l_f + v_{y,k}}{v_{x,k}} \right) \quad (10)$$

$$\alpha_{r,k} = - \left(\frac{v_{y,k} - \dot{\psi}_k l_r}{v_{x,k}} \right) \quad (11)$$

The longitudinal acceleration was incorporated into the *NN* structure with the aim to predict the lateral force reduction during combined longitudinal and lateral solicitations (force coupling), thus permitting an accurate vehicle state estimation in non-constant speed events (e.g. braking in a turn). It is important to remark that this approach considers a quasi-static weight transfer in the longitudinal direction, and an even surface. Road irregularities will be addressed in future stages of this research. The datasets necessary to train the *NN* structure

were generated in *IPG-CarMaker*® using an experimentally validated compact-class vehicle model [3] and a state-of-the-art Magic Formula 6.1 tire model [24]. Open Loop aggressive maneuvers (Step steer) covering different longitudinal acceleration levels (Braking, Power On) were simulated for this purpose. Finally, the *NN* was trained in *Matlab*® using the Levenberg-Marquardt backpropagation algorithm and a 70/15/15% dataset division was selected after performing a sensitivity analysis. The stability of the *NN* structure was studied following the methodology described in [25]. For additional details regarding the application of *NN* to model the tire friction forces, [3] can be consulted.

D. Extended Kalman Filter

In order to present the *EKF*, it is necessary to adopt the state-space formulation. The vehicle dynamics equations (1-3) can be expressed in state-space form by the set of discrete equations (12-13):

$$X_{k+1} = f(X_k, U_k) + w_k \quad (12)$$

$$Y_k = h(X_k) + v_k \quad (13)$$

In this system, the terms $f(\cdot)$ and $h(\cdot)$ denote the state evolution and observation vectors respectively. The system states, system inputs and system outputs are represented by the vectors X_k , U_k and Y_k . The plant uncertainties are modeled by the variable w_k , whereas v_k is employed to model the noise associated with the system outputs. These noises are assumed to be Gaussian, uncorrelated and zero mean, i.e. ($w \approx N(0, Q)$, $v \approx N(0, R)$). The plant and measurement covariance matrices are noted by Q and R respectively. Following the formulation presented in [9], the *EKF* action can be subdivided into the *time update* and *measurement update* steps, represented by the expressions (14-18).

Time update

$$\hat{X}_{k|k-1} = f(\hat{X}_{k-1|k-1}, U_k) \quad (14)$$

$$P_{k|k-1} = A_k P_{k-1|k-1} A_k^T + Q \quad (15)$$

Measurement update

$$K_k = P_{k|k-1} H_k^T [H_k P_{k|k-1} H_k^T + R]^{-1} \quad (16)$$

$$\hat{X}_{k|k} = \hat{X}_{k|k-1} + K_k [Y_k - h(\hat{X}_{k|k-1})] \quad (17)$$

$$P_{k|k} = [I - K_k H_k] P_{k|k-1} \quad (18)$$

During the first stage of the algorithm, the plant model (a priori knowledge of the system) is used to predict the system states in the next time step (14). The covariance matrix $P_{k|k-1}$ is calculated using the process covariance matrix Q , and the jacobian matrix of the state evolution vector A_k , expression (15). After that, the predicted states $\hat{X}_{k|k-1}$ are corrected in the *measurement update* stage. The filter gain K_k is computed from the predicted covariance matrix $P_{k|k-1}$, the measurement covariance matrix R , and the jacobian of the observation vector H_k , equation (16). Once the filter gain is calculated, the measurement residuals are used to correct the states predicted in the *time update* stage, expression (17). Finally, the covariance matrix is updated, expression (18).

E. Observability of the EKF

In this paper, the Lie Derivative was used to study the local observability of the system [9]. Lack of observability is present during null longitudinal velocity, and the observer is switched off each time the vehicle velocity goes below 2.7 m/s to avoid the ill-conditioning of the system. For further details, [3] can be consulted.

III. OBSERVER TUNING

A. Contrast-based Fruit Fly Optimization

Fruit flies are very efficient in detecting food as they can locate it, even if this is 40 km away. Pan, inspired by fruit flies' foraging behavior, proposed for the first time a Fruit Fly Optimization (*FOA*) algorithm on this basis [26]. The authors have developed an enhanced version of the original *FOA* [19], which includes the following steps; for simplification, the routine is presented for a one-dimensional optimization problem:

Algorithm 1 Contrast-based Fruit Fly Optimization

- **Step 1: Initialization.** The average swarm location $[x_0, y_0]$, the maximum number of iterations K , the size of the swarm N , the delay κ , the scaling factor M , and the contraction parameter c are defined.
- **Step 2: Swarm Generation.** A new population of fruit flies $[x_i, y_i]$ of length (N), is created through the following randomized process:

$$x_i = x_0 \cdot (1 + M_i \cdot (2 \cdot \text{rand} - 1)) \quad (19)$$

$$y_i = y_0 \cdot (1 + M_i \cdot (2 \cdot \text{rand} - 1)) \quad (20)$$
- **Step 3: Localization.** Each fruit fly is assigned a value S_i based on how close the fly $[x_i, y_i]$ is to the origin:

$$d_i = \sqrt{x_i^2 + y_i^2} \quad (21)$$

$$S_i = \frac{1}{d_i} \quad (22)$$
- **Step 4: Smell concentration/ Objective function calculation.** The corresponding smell concentration for each fruit fly i is defined, where f is the objective function.

$$\text{Smell}_i = f(S_i) \quad (23)$$
- **Step 5: Best member identification.** The fruit fly with the highest smell concentration (S_b) in the swarm and its location (x_b, y_b) are identified:

$$\text{Smell}_b = \max(\text{Smell}_i) \quad (24)$$
- **Step 6: Average location selection.** The best fruit fly is compared to the existing average location:

$$\text{if } \text{Smell}_b > \text{Smell}_0, \quad (25)$$

$$x_0 = x_b, y_0 = y_b$$
- ❖ **Condition 1:**
 - If the maximum number of iterations K has been reached *then* terminate the optimization process, retrieve the optimal fruit fly S_{opt} as well as the corresponding objective function value Smell_{opt} .

- Else, continue to Step 7.
- **Step 7: Decision delay.** In this phase, the fruit fly swarm does not change its food search strategy for κ iterations. This resembles the delay in decision-making that also fruit flies exhibit.
- ❖ **Condition 2:**
 - If the smell concentration $Smell_0$ improves over the last κ iterations, then go to step 8a.
 - Else if the smell concentration $Smell_0$ does not change over the last κ iterations, then go to step 8b.
 - If the smell concentration $Smell_0$ worsens over the last $2 \cdot \kappa$ iterations, then go to step 8c.
- **Step 8a: Casting.** Go to Step 2 without any change.
- **Step 8b: Visual feature detection.** The fruit fly with the worst smell concentration $Smell_w$ is identified and the fruit fly swarm becomes attracted to it. Reduce the scale factor M and go to Step 2.

$$[x_w \ y_w] \rightarrow Smell_w = \min(Smell_i) \quad (26)$$

$$x_0 = x_w \text{ and } y_0 = y_w \quad (27)$$

$$M_{i+1} = 0.9 \cdot M_i \quad (28)$$

where i is the current iteration. Eventually, the flies will explore the area around the fruit fly with $Smell_w$. This resembles the visual cue fruit fly search behavior.
- **Step 8c: Reset.** Return to the location that encountered the best smell concentration $Smell_0$ up to that point. Then go to Step 2.

$$x_0 = x_b \text{ and } y_0 = y_b \quad (29)$$

This resembles the memory function that fruit flies present.

B. Objective function formulation

In this study, the objective function is formulated as the weighted average of the combination of longitudinal velocity, lateral velocity, yaw rate and lateral acceleration errors (30).

$$Smell = \sum_{j=1}^{Nsam} \left(w_1 \cdot (\hat{v}_{x,j} - v_{x,j})^2 + w_2 \cdot (\hat{v}_{y,j} - v_{y,j})^2 + w_3 \cdot (\hat{\psi}_j - \psi_j)^2 + w_4 \cdot (\hat{a}_{y,j} - a_{y,j})^2 \right) \quad (30)$$

Where w_1, w_2, w_3 and w_4 are user defined parameters. The lateral acceleration is obtained from the vehicle motion states as (31), and $Nsam$ is the number of data samples

$$a_y = \dot{\psi} \cdot v_x - dv_y/dt \quad (31)$$

In this paper, $w_1=w_2=w_3=w_4 = 0.25$. Thus, the *EKF* tuning problem is formulated as an optimization problem for which the design parameters Q^*, R^* are sought that minimize the objective function:

$$Q^*, R^* \rightarrow \min(Smell) \quad (32)$$

IV. RESULTS

The state estimator described in Section II was constructed in *Simulink*® and integrated into the vehicle dynamics simulation software *IPG-CarMaker*®. The discretization time was set to 1ms, and the measurable quantities were acquired at a frequency of 100Hz using a zero-order hold block. An additive white Gaussian noise model was used to incorporate the uncertainties associated with the measurement equipment in the simulation signals [27,28].

A. EKF Optimization

The diagonal terms of the *EKF* covariance matrices (Q, R) were tuned following the methodology presented in Section III. An optimization dataset was formed by concatenation of Lane Change, Slalom and Sine with Dwell maneuvers (tests #1, #3, #6, #7, Table I), Fig. 3, and the design parameters (Q^*, R^*) which minimized the objective function (32) were found.

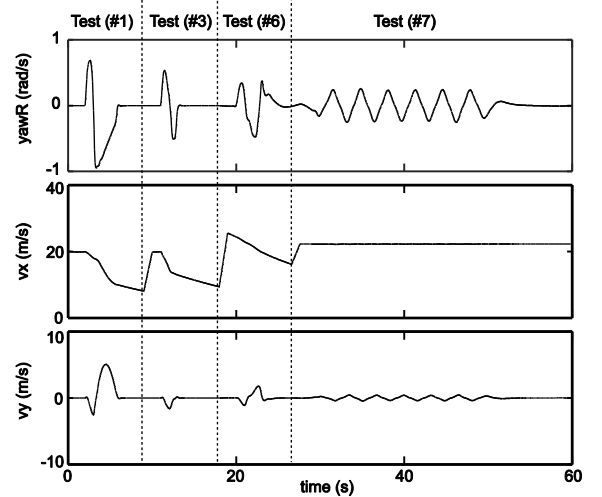


Fig. 3. Optimization dataset, Tests #1, #3, #6, and #7.

B. Evaluation of the Optimized Observer

The catalog of maneuvers presented in Table I was simulated to test the performance of the optimized observer. Additional maneuvers (#2, #4, #5, #8) were added in order to check the suitability of the observer under scenarios not included in the optimization dataset. The nomenclature *base* is used to note the results obtained with a preliminary filter tuning carried out manually [3]. The normalized *RMS* errors [3,9] of the optimized observer were calculated for each test and presented in Table II.

TABLE I. CATALOG OF MANEUVERS. **CD**: COAST DOWN, **PB**: PARTIAL BRAKING, **HB**: HARD BRAKING, **MS**: MAINTAIN SPEED.

Test	Speed / SWA / Braking input
#1 Sine with Dwell	80kph / 150° / CD
#2 Sine with Dwell	80kph / 90° / CD
#3 Sine with Dwell	80kph / 90° / PB
#4 Sine with Dwell	80kph / 70° / HB
#5 ISO Lane Change	100kph / - / MS
#6 ADAC Lane Change	100kph / - / CD
#7 Slalom 36m	80kph / - / MS
#8 Slalom 18m	60kph / - / MS

Overall, the errors keep within a 10% of accuracy for the majority of the maneuvers tested. Largest errors are observed in the front axle forces estimated during the test number 4 (Sine with Dwell with Hard Braking). Despite this, the normalized error of the lateral velocity is acceptable. In order to check the relative improvement of the optimized filter with respect to the *base* configuration, the error increment (Δe) was calculated using the equation (33).

$$\Delta e = 100 \frac{e_{base} - e_{opt}}{e_{base}} \quad (33)$$

The results are presented in Fig. 4. The noise reduction achieved with the optimization of the filter is remarkable and ranges between 20 to 60 percent in all the tests except in the maneuver number 4. In this last, the lateral velocity error increases due to the uncertainty associated with the front axle lateral forces during hard braking. Nevertheless, the absolute value of the lateral velocity error is roughly 6 percent and can be accepted.

TABLE II. NORMALIZED RMS ERROR.

Test	e_{ψ}	e_{v_x}	e_{v_y}	e_{a_y}	$e_{F_{yf}}$	$e_{F_{yr}}$
#1	1.68	0.62	1.69	3.54	4.07	4.23
#2	1.78	0.61	2.18	2.32	2.20	4.24
#3	2.22	0.63	4.69	4.66	4.99	7.41
#4	1.37	0.72	6.37	10.40	17.22	6.25
#5	2.16	0.62	2.60	2.61	2.81	3.41
#6	1.94	0.54	2.18	1.83	2.10	4.08
#7	2.84	0.57	6.26	1.76	1.82	3.22
#8	2.25	0.64	4.25	3.36	2.62	6.51

The improvement introduced by the optimized state estimator is particularly noticeable in the test number 8 (Slalom 18 meters), where a systematic reduction in the noise level is seen in all the estimated vehicle states and axle forces.

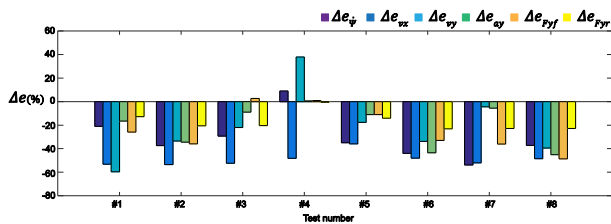


Fig. 4. Relative improvement of the optimized observer.

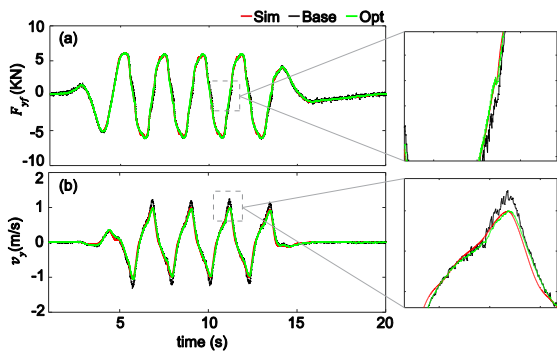


Fig. 5. (a) Front lateral force, (b) lateral velocity. Test #8.

The time histories of the front axle lateral force and the lateral velocity obtained during the simulation of this test are presented in Fig. 5. Apart from the expected reduction in the noise level, the optimized state estimator is able to approximate the simulation signals with high accuracy, thus eliminating the offset (lateral velocity) and delay (front axle lateral force) exhibited by the *EKF* tuned with the *base* configuration.

V. CONCLUSIONS

The results presented in this paper evidence the suitability of the contrast-based Fruit Fly Optimization algorithm as a robust and efficient approach to tune an Extended Kalman Filter. The reduction in the error of the estimated vehicle states and tire forces is significant, and the time-consuming task of manually tuning the filter is eliminated.

The approach presented in this paper can reduce drastically the development time of automotive control systems. This can be especially advantageous when dealing with systems that present systematic errors and require an optimal tuning for each particular situation.

In the following stages of this research, the performance of this optimization approach will be assessed in other nonlinear state estimators (Unscented Kalman Filter). Moreover, the determination of the optimum filter values for particular driving situations (e.g. steady-state driving, transient driving) as well as the subsequent integration in a covariance-scheduled scheme will be pursued.

ACKNOWLEDGMENT

This project has received funding from the European Unions Horizon 2020 research and innovation program under the Marie Skłodowska-Curie grant agreement No: 675999. M. E. Fitzpatrick is grateful for funding from the Lloyd's Register Foundation, a charitable foundation helping to protect life and property by supporting engineering-related education, public engagement and the application of research.

REFERENCES

- [1] M. Alirezaei, S. Kanarachos, B. Scheepers and J. P. Maurice, "Experimental evaluation of optimal Vehicle Dynamic Control based on the State-Dependent Riccati Equation technique," 2013 American Control Conference, Washington, DC, 2013, pp. 408-412. doi: 10.1109/ACC.2013.6579871
- [2] S. Kanarachos, A. Kanarachos, "Intelligent road adaptive suspension system design using an experts' based hybrid genetic algorithm." Expert Systems with Applications, 2015, 42, pp. 8232-8242
- [3] M. Acosta, S. Kanarachos, "Tire force estimation and road grip recognition using Extended Kalman Filter, Neural Networks and Recursive Least Squares", submitted to Neural Computing and Applications, Springer, (under review), 2017.
- [4] V. Ivanov, D. Savitski, "Systematization of Integrated Motion Control of Ground Vehicles." IEEE Access, 2015, 3, pp. 2088-2099.
- [5] J. Eom, H. Lee, B. Choi, "A study on the tire deformation sensor for intelligent tires". International Journal of Precision Engineering and Manufacturing, 2014, 15(1), pp.155-160.
- [6] R. Matsuzaki, T. Keating, A. Todoroki, N. Hiraoka, "Rubber-based strain sensor fabricated using photolithography for intelligent tires". Sensors and Actuators A: Physical, 2008, 148(1), pp.1-9.
- [7] R. Matsuzaki, A. Todoroki, "Wireless Monitoring of Automobile Tires for Intelligent Tires". Sensors, 2008, 8(12), pp.8123-8138

- [8] K. Singh, S. Taheri, "Estimation of tire-road friction coefficient and its application in chassis control systems". *Systems Science & Control Engineering*, 2014, 3(1), pp.39-61
- [9] M. Doumiati, A. Charara, A. Victorino, D. Lechner, "Vehicle Dynamics Estimation using Kalman filtering," Wiley, 2012, DOI: 10.1002/9781118578988
- [10] S. Burkul, P. R. Pawar, K. Jagtap, "Estimation of Vehicle Parameters using Kalman Filter: Review", *International Journal of Current Engineering and Technology*, 2014, 4(4)
- [11] K. György, A. Kelemen, L. Dávid, "Unscented Kalman Filters and Particle Filter Methods for Nonlinear State Estimation", *Procedia Technology*, 2014, 12, pp.65-74.
- [12] P. Dixon, M. Best, T. Gordon, "An Extended Adaptive Kalman Filter for Real-time State Estimation of Vehicle Handling Dynamics". *Vehicle System Dynamics*, 2000, 34(1), pp.57-75.
- [13] L. Li, G. Jia, X. Ran, J. Song, K. Wu, "A variable structure extended Kalman filter for vehicle sideslip angle estimation on a low friction road". *Vehicle System Dynamics*, 2014, 52(2), pp.280-308
- [14] C. Zhou, J. Xiao, H. Sheng, "Application of multi-rate EKF soft computing in vehicle state estimation". *Journal of Electronic Measurement and Instrument*, 2013, 26(2), pp.132-137
- [15] J. Valappil, C. Georgakis, "Systematic estimation of state noise statistics for extended Kalman filters". *AIChE Journal*, 2000, 46(2), pp.292-308
- [16] N. Kaur, A. Kaur, "A Review on Tuning of Extended Kalman Filter using Optimization Techniques for State Estimation". *International Journal of Computer Applications*, 2016, 145(15), pp.1-5
- [17] N. Kaur, A. Kaur, "Tuning of Extended Kalman Filter for Nonlinear State Estimation". *IOSR Journal of Computer Engineering*, 2016, 18(05), pp.14-19
- [18] L. Scardua, J. da Cruz, "Automatic Tuning of the Unscented Kalman Filter and the Blind Tricyclist Problem: An Optimization Problem". *IEEE Control Systems*, 2016, 36(3), pp.70-85.
- [19] S. Kanarachos, J. Griffin, M. Fitzpatrick, "Efficient truss optimization using the contrast-based fruit fly optimization algorithm". *Computers & Structures*, 2016, 182, pp.137-148
- [20] S. Melzi, E. Sabbioni, "On the vehicle sideslip angle estimation through neural networks: Numerical and experimental results". *Mechanical Systems and Signal Processing*, 2011, DOI: 10.1016/j.ymssp.2010.10.015
- [21] M. Hrgetic, J. Deur, V. Ivanovic, E. Tseng, "Vehicle sideslip angle EKF Estimator based on Nonlinear Vehicle Dynamics Model and Stochastic Tire Forces Modeling", *SAE International Journal of Passenger Cars*, 2014, DOI: 10.4271/2014-01-0144
- [22] S. Kanarachos, "Design of an Intelligent Feed Forward controller system for vehicle obstacle avoidance using Neural Networks." *International Journal of Vehicle Systems Modelling and Testing*, 2013, 8 (1), pp. 55-87
- [23] S. Kanarachos, "A new min-max methodology for computing optimized obstacle avoidance steering maneuvers of ground vehicles." *International Journal of Systems Science*, 2014, 45 (5), pp. 1042-1057
- [24] H.B. Pacejka, "Tire and Vehicle Dynamics", Butterworth-Heinemann, 2012, DOI: 10.2307/3885338
- [25] I. Belic, "Neural Networks and Static Modelling," *Recurrent Neural Networks and Soft Computing*, 2012, Dr. Mahmoud ElHefnawi
- [26] W. Pan, "A new Fruit Fly Optimization Algorithm: Taking the financial distress model as an example". *Knowledge-Based Systems*, 2012, 26, pp.69-74
- [27] RaceLogic, "Vbox 3i *GPS System Technical Datasheet*", 2015
- [28] RaceLogic, "RLVBIMU04 IMU *Technical Datasheet*", 2015